Circulation: Cardiovascular Imaging

ORIGINAL ARTICLE

Impact of Ventricular Morphology on Fiber Stress and Strain in Fontan Patients

See Editorial by Helbing

Sunil J. Ghelani, MD
Steven D. Colan, MD
Nina Azcue, BS
Ellen M. Keenan, BS
David M. Harrild, MD, PhD
Andrew J. Powell, MD
Tal Geva, MD
Rahul H. Rathod, MD

BACKGROUND: Right ventricular (RV) morphology has been associated with adverse clinical outcomes in Fontan patients. The impact of RV versus left ventricular morphology on ventricular stress and strain in single ventricles is not well known.

METHODS AND RESULTS: Cardiac magnetic resonance examinations in 193 patients with the Fontan circulation were retrospectively analyzed. Ventricular mass, volume, global circumferential and longitudinal strain, and global average end-systolic fiber stress were calculated using previously published methods. Compared with left ventricular morphology, RV morphology (48%) was associated with higher ventricular end-diastolic volume (110 mL/BSA$^{1.3}$ versus 84 mL/BSA$^{1.3}$, P<0.001), lower mass-to-volume ratio (0.46 versus 0.57, P<0.001), higher global average end-systolic fiber stress (23 kPa versus 20 kPa, P=0.002), worse global circumferential strain (–21% versus –24%, P<0.001), and higher prevalence of greater than or equal to moderate atrioventricular valve regurgitation (25% versus 6%, P<0.001). Ejection fraction and global longitudinal strain were similar between the groups. Death or listing for heart transplantation occurred in 24 (12%) with a median follow-up of 6.2 years. On univariate analysis, RV morphology, ventricular dilatation, and worse global circumferential strain were associated with this composite outcome.

CONCLUSIONS: In comparison to Fontan patients with a dominant left ventricle, those with a dominant RV have higher fiber stress, a higher rate of ventricular dilatation, lower circumferential fiber shortening, and similar longitudinal shortening. RV morphology, ventricular dilation, and worse circumferential strain are associated with death or heart transplantation. The difference in myofiber architecture may contribute to suboptimal adaptation of the RV as a systemic ventricle.

Key Words: blood pressure ■ dilatation ■ heart transplantation ■ prevalence

http://circimaging.ahajournals.org

CLINICAL PERSPECTIVE

The anatomic left and right ventricles have inherent differences including differences in myofiber architecture. The right ventricle adapts suboptimally as a solitary pumping chamber in the Fontan circulation as compared with the left ventricle. This cardiac magnetic resonance imaging-based study showed that in the Fontan circulation, single right ventricles have a higher end-systolic wall and fiber stress, a higher rate of ventricular dilation, lower circumferential fiber shortening, and similar longitudinal shortening as single left ventricles. Ventricular dilation, worse circumferential strain, and right ventricular morphology are associated with death or transplantation in this population.

A Fontan operation is the typical final palliative surgery for patients with a functional single ventricle. The abnormal hemodynamic load associated with the Fontan circulation leads to remodeling of the single ventricle, but given the intrinsic and structural differences between morphological right ventricle (RV) and left ventricle (LV), it is reasonable to expect the LV to adapt better as a systemic ventricle than the RV. For example, in a biventricular circulation after a Mustard or Senning operation for transposition of the great arteries, the RV has a high rate of decompensation in young adults.[1,2] Several publications in the Fontan literature suggest worse clinical outcomes in RV dominant hearts compared with LV, but the mechanisms for this observation remain unclear.[3–12]

The physiological variables that affect ventricular function and its adaptation are preload, afterload, and contractility. Invasive measurements with high fidelity pressure and volume catheters are required to obtain an accurate assessment of these variables. Noninvasive indices are often used as approximates for ventricular preload (eg, cavity dimension, volume), afterload (eg, blood pressure, wall, or fiber stress), and contractility (eg, ejection fraction [EF], shortening fraction, strain). Cardiac magnetic resonance (CMR) based methods to estimate ventricular stress and strain have been developed and previously reported in structurally normal hearts.[13,14] However, these measurements and their interrelationships have not been explored in detail in patients with single ventricles.

The present study aimed to noninvasively measure ventricular fiber stress and strain in Fontan patients using CMR and hypothesized that RVs may have higher fiber stress and lower global strain compared with LVs. In addition, the study evaluated associations between ventricular morphology and clinical outcomes, including cardiopulmonary exercise testing data, heart transplantation, and death.

METHODS

The data, analytic methods, and study materials will not be made publicly available to other researchers for purposes of reproducing the results or replicating the procedure.

Study Population

Patients with Fontan circulation who underwent a CMR examination between August 2003 and February 2016 at our center were retrospectively identified. When multiple studies were available for a patient, the most recent study was used for analysis. Ventricular morphology was categorized as LV, RV, or mixed. The mixed category was applied when a significant sized smaller ventricle (defined as end-diastolic volume [EDV] ≥25% of combined ventricular EDV or EDV Z score ≥−4) contributed to the systemic circulation, and these patients were excluded from further analysis. Minimum requirements for further analysis included availability of ventricular mass and volume data from the CMR, availability of an upper extremity cuff blood pressure, and the ability to perform feature tracking analysis in at least one plane.

CMR Protocol

Studies were performed on a 1.5 Tesla scanner (Philips Healthcare, Best, the Netherlands). The details of the CMR protocols used in our unit for assessment of patients after the Fontan operation have been previously published.[15,16] A stack of electrocardiographic-gated, breath-hold steady-state free precession cine images acquired in a ventricular short-axis plane were used for ventricular mass, volume, and feature tracking analysis. Typical spatial resolution was 1.7 to 2 mm by 1.7 to 2 mm with a slice thickness of 8 mm. For each slice, 30 phases were reconstructed with a typical temporal resolution of 30 to 40 ms. Ventricular mass, volumes, and EF were measured by manually tracing endocardial and epicardial borders at end-diastole (maximal area) and end-systole (minimum area) using commercially available software (QMass, Medis Medical Imaging Systems, Leiden, the Netherlands). Variables included indexed ventricular EDV (EDV_i), indexed end-systolic volume (ESV_i), EF, end-diastolic epicardial volume (EDV_{epi}), myocardial volume, indexed ventricular mass ($Mass_i$), and mass-to-volume ratio. Myocardial volume was defined as the difference between epicardial and cavity volumes (EDV_{epi}−EDV). Mass and volume measurements were indexed to BSA[1.3].[15,17] When 2 ventricles contributed to the systemic circulation, total biventricular volume and mass were used. Flow measurements were performed using an electrocardiographically gated through-plane cine phase-contrast magnetic resonance sequence. Target vessels included the ascending aorta, superior and inferior venae cavae, right and left pulmonary artery branches, and individual right and left pulmonary veins. Blood flow rates were calculated using commercially available software (QFlow, Medis Medical Imaging Systems, Leiden, the Netherlands). Aortopulmonary collateral flow was quantified as the difference between ascending aortic flow and the total systemic venous return as previously described.[18,19] When available,

the degree of atrioventricular valve (AVV) regurgitation and aortic regurgitation was categorized as significant (greater than or equal to moderate or a regurgitation fraction ≥20%) and not significant (mild or lower).

Stress Analysis

Two measures of ventricular stress were calculated (1) end-systolic wall stress (ESWS) and (2) global average midwall end-systolic fiber stress ($ESFS_{ga}$).[13,20,21] For both measurements, mean upper extremity cuff blood pressure (typically recorded immediately before or after the CMR) was used as a surrogate for ventricular end-systolic pressure.[22] ESWS was calculated using the thick-walled spherical model that estimates wall stress inside a hypothetical sphere with a cavity volume equal to ventricular ESV, and wall volume equal to ventricular muscle volume by the following formula.[13,20]

$$ESWS = \frac{MBP}{\left(\frac{ESV + \text{Myocardial volume}}{ESV}\right)^{2/3} - 1}$$

MBP=mean Blood Pressure (kPa), ESV=end-systolic volume (mL).

$ESFS_{ga}$ was calculated using the following formula as described by Regen et al.[21]

$$ESFS_{ga} = \frac{1.5 \times \left(ESV + \left(\frac{EDV_{epi} \times EDV \times \left(Ln\left(EDV_{epi}\right) - Ln\left(EDV\right)\right)}{\text{Myocardial volume}} - EDV \right) \right)}{EDV - \frac{EDV_{epi} \times EDV \times \left(Ln\left(EDV_{epi}\right) - Ln\left(EDV\right)\right)}{\text{Myocardial volume}}} \times MBP}{Ln\left(EDV_{epi}\right) - Ln\left(EDV\right)}$$

MBP=mean blood pressure (kPa), ESV=end-systolic volume (mL), EDV=end-diastolic volume (mL), EDV_{epi}=epicardial end-diastolic volume (mL).

Strain Analysis

Global circumferential strain (GCS) and global longitudinal strain (GLS) were calculated using feature tracking analysis on the steady-state free precession ventricular short-axis and 4-chamber images at the midcavity level using commercially available software (2D CPA MR, version 1.1.2.36, TomTec imaging systems, Unterschleissheim, Germany). Details of the strain analysis methodology and reproducibility in our laboratory have been previously published.[23] The endocardial border of the single (or dominant) ventricle was manually traced, and the software automatically tracked the border throughout the cardiac cycle. If tracking was judged to be suboptimal by visual inspection, the endocardial border was retraced until satisfactory tracking was accomplished. As GCS and GLS represent fiber shortening, they have a negative numeric value. Throughout the article, a numerically lower (more negative) value represents greater shortening and is referred to as better GCS/GLS, whereas a numerically higher value (less negative) is referred to as worse GCS/GLS.

Cardiac Catheterization Data

When available, and if performed within 2 years of the CMR, results of cardiac catheterization were reviewed. Catheterizations with interim surgical interventions were excluded.

Outcomes

When available, and if performed within 2 years of the CMR, results of a cardiopulmonary exercise test were reviewed for the following variables: percent predicted peak rate of oxygen consumption (Vo_2), percent predicted work rate, and ventilatory equivalent for oxygen (VE/Vco_2 slope). Exercise tests with submaximal effort (respiratory exchange ratio <1.09 or heart rate <70% predicted) were excluded.

Medical records were reviewed for a composite outcome that included all-cause mortality, heart transplantation, or listing for heart transplantation. Dates of listing for cardiac transplantation, transplantation, or death were confirmed against the New England Organ Bank and the Social Security Death Index databases. Follow-up was measured from the date of the CMR to the above outcome or the last known follow-up date.

Statistical Analysis

Continuous variables are reported as medians with interquartile ranges unless otherwise specified. Continuous measurements were compared between the LV and RV groups using the Mann-Whitney *U* test. Proportions were compared using the Fisher exact test. Univariate and multivariable regressions were performed to explore presence of linear relationships between various measurements in the overall cohort as well as subgroup analysis within each of the 2 morphology groups. Slopes of ventricular stress-strain relationship between LV and RV groups (as depicted in Figure 1) were compared using ANOVA incorporating factor-by-covariate interaction terms.[24] Kaplan Meier survival curves with log-rank test were used to compare freedom from the composite outcome between LV and RV groups (analysis was restricted to 10 years of follow-up because of sparse data and unreliable estimates beyond that period). Analyses were performed using SPSS version 21.0 (IBM Corporation, Armonk, New York) and STATA/SE 13.1 (StataCorp LP, College Station, TX).

The Boston Children's Hospital Committee on Clinical Investigation approved this study and waived the requirement for informed consent.

RESULTS

Baseline Characteristics

A total of 334 patients met the initial screening criteria. Of these, 105 were excluded because of mixed ventricular morphology and further 36 were excluded because of suboptimal imaging data or lack of blood pressure measurement. Hence, the study population included 193 patients (63% male) with a median age of 16 (11–23) years (Table 1). The LV group included 101 (52%) patients and the RV group included 92 (48%) patients. Patients in the RV group were younger and had a lower mean blood pressure when compared

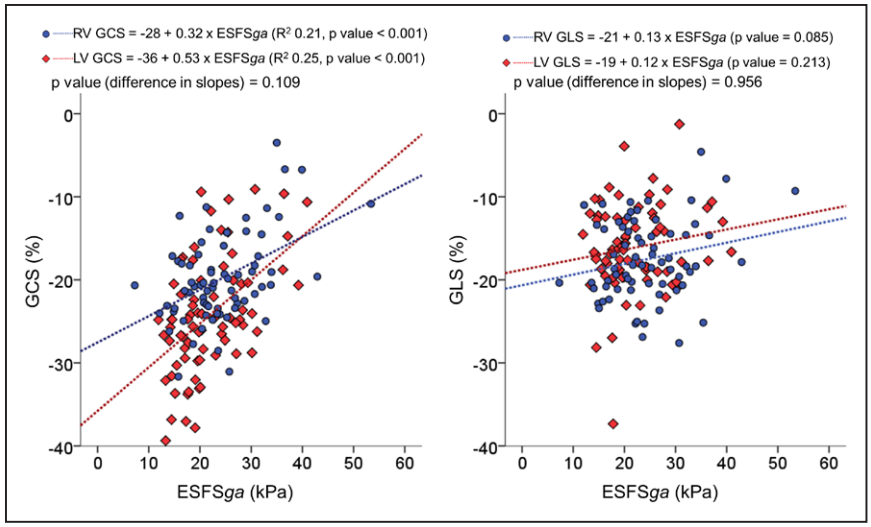

Figure 1. Ventricular stress-strain relationship stratified by ventricular morphology. Scatter plots and linear regression lines depicting relationship between global circumferential strain (GCS; **left**), global longitudinal strain (GLS; **right**), and global average midwall end-systolic fiber stress ($ESFS_{ga}$). LV indicates left ventricle; and RV, right ventricle.

with the LV group. The most common anatomic diagnoses were hypoplastic left heart syndrome (32%), tricuspid atresia (21%), double-inlet LV (19%), double-outlet RV (9%), pulmonary atresia with intact ventricular septum (7%), unbalanced common atrioventricular canal defect (5%), and hypoplastic right heart structures (3%).

CMR Findings

Table 2 shows comparisons of mass, volumes, function, flow, stress, and strain data between the RV and LV groups. Compared with the LV group, patients with single RV had larger ventricular diastolic and systolic volumes, higher wall and fiber stress despite a lower mean blood pressure, a higher proportion of AVV regurgitation, lower mass-to-volume ratio, and worse GCS. The effect of ventricular morphology on GCS and $ESFS_{ga}$ was independent of age on multivariate regression analysis. $ESFS_{ga}$ showed a significant negative correlation with EF (R^2=0.45, P<0.001) but no relationship with age (P=0.410) or body surface area (P=0.332). There was a weak but statistically significant linear correlation between aortopulmonary collateral flow and EDV_i (R^2=0.07, P=0.006) as well as $ESFS_{ga}$ (R^2=0.05, P=0.019). Patients with greater than or equal to moderate AVV regurgitation (n=25) were more likely to have dilated ventricles (EDV_i 131 [103–202] mL/$BSA^{1.3}$ versus

Table 1. Patient Characteristics

	All Patients (n=193)	RV Group (n=92)	LV Group (n=101)	*P* Value
Age at Fontan, y	3 (2.2–4.9)	2.7 (2.2–4.1)	3.4 (2.5–5.8)	0.083
Age at CMR, y	16 (10–23)	14 (9–20)	18 (13–25)	0.017*
BSA, m^2	1.5 (1.1–1.8)	1.5 (0.9–1.7)	1.6 (1.2–1.8)	0.347
Heart rate, bpm	83 (70–95)	85 (73–95)	80 (68–90)	0.223
Mean BP, mm Hg	76 (69–84)	74 (67–82)	79 (72–86)	0.005*
Prior shunt type				
Blalock-Taussig shunt	130 (67%)	62 (67%)	68 (67%)	1.000
RV-PA conduit	9 (5%)	9 (10%)	0 (0%)	0.001*
Central shunt	7 (4%)	4 (4%)	3 (3%)	0.711
No shunt	36 (19%)	14 (15%)	22 (22%)	0.271
Mixed	11 (6%)	3 (3%)	8 (8%)	
Type of Fontan operation				
Lateral tunnel	152 (79%)	75 (82%)	77 (76%)	0.385
RV-PA anastomosis	22 (11%)	7 (8%)	15 (15%)	0.173
Extracardiac conduit	15 (8%)	9 (10%)	6 (6%)	0.422
Others	4 (2%)	1 (1%)	3 (3%)	

Values are medians (interquartile range) or count (%). BP indicates blood pressure; BSA, body surface area; CMR, cardiac magnetic resonance; LV, left ventricle; PA, pulmonary artery; and RV, right ventricle.
*Indicates P<0.05.

Table 2. Comparison of CMR Data Between RV and LV Groups

	All Patients		RV group		LV group		*P* Value
	n		n		n		
EDV_i, mL/BSA$^{1.3}$	193	93 (77 to 119)	92	110 (83 to 133)	101	84 (73 to 109)	<0.001*
ESV_i, mL/BSA$^{1.3}$	193	44 (33 to 64)	92	49 (36 to 73)	101	39 (29 to 53)	<0.001*
$Mass_i$, gram/BSA$^{1.3}$	193	50 (41 to 61)	92	49 (42 to 63)	101	50 (41 to 59)	0.722
Mass-to-volume ratio	193	0.52 (0.43 to 0.63)	92	0.46 (0.39 to 0.56)	101	0.57 (0.48 to 0.68)	<0.001*
EF, %	193	54 (47 to 59)	92	53 (47 to 58)	101	55 (47 to 60)	0.347
ESWS, kPa	193	16 (13 to 22)	92	18 (14 to 24)	101	15 (12 to 20)	0.002*
$ESFS_{ga}$, kPa	193	21 (18 to 27)	92	23 (18 to 29)	101	20 (17 to 25)	0.002*
APC flow, L/min per m^2	105	0.6 (0.3 to 1.3)	51	0.8 (0.3 to 1.5)	54	0.5 (0.3 to 1.1)	0.205
≥ moderate AR	6/157	3.8%	2/76	2.6%	4/81	4.9%	0.682
≥ moderate AVVR	25/167	15%	20/82	24.4%	5/85	5.9%	<0.001*
Cardiac index, L/min per m^2	147	4.4 (3.5 to 5.7)	72	4.6 (3.6 to 6.2)	75	4.2 (3.5 to 5.4)	0.565
GCS, %	144	−17 (−20 to −13)	70	−21 (−14 to −17)	74	−25 (−29 to −20)	<0.001*
GLS, %	140	−17 (−20 to −13)	69	−18 (−21 to −14)	71	−17 (−19 to −13)	0.310

Values are medians (interquartile range) or as percentages. APC indicates aortopulmonary collateral flow; AR, aortic regurgitation; AVVR, atrioventricular valve regurgitation; CMR, cardiac magnetic resonance; EDV_i, indexed ventricular end-diastolic volume; EF, ejection fraction; $ESFS_{ga}$, global average midwall end-systolic fiber stress; ESV_i, indexed ventricular end-systolic volume; ESWS, end-systolic wall stress; GCS, global circumferential strain; GLS, global longitudinal strain; LV, left ventricle; $Mass_i$, indexed ventricular mass; and RV, right ventricle.

*Indicates $P<0.05$

89 [76–113] mL/BSA$^{1.3}$, $P<0.001$). Presence of greater than or equal to moderate AVV regurgitation was also associated with a worse GCS (−19% [−23% to −12%] versus −23% [−26% to −19%], $P=0.025$), and higher $ESFS_{ga}$ (30 [25–33] kPa versus 20 [17–25] kPa, $P<0.001$).

Both measures of ventricular stress (ESWS and $ESFS_{ga}$) were calculated using different mathematical equations based on the same set of variables and showed excellent correlation (Figure 2). Ventricular stress-strain relationships stratified by ventricular morphology are depicted in Figure 1. There was a significant linear decline in GCS with increased $ESFS_{ga}$ in both RV and LV groups; however, the relationship between GLS and $ESFS_{ga}$ did not achieve statistical significance in either group.

Subgroup analysis of the RV group showed that dilated RVs (EDV_i ≥100 mL/BSA$^{1.3}$; n=40) had a worse GCS as compared with the rest of the RV group (−19% [−22% to −14%] versus −23% [−24% to −21%], $P<0.001$) but similar GLS (−17% [−20% to −13%] versus −18% [−21% to −16%], $P=0.155$).

Catheterization Findings

Cardiac catheterization data were available in 70 patients (38 RV, 32 LV). The median gap between the catheterization and CMR was 49 (1–268) days. The median Fontan baffle pressure was 15 (12–17) mm Hg, cardiac index was 3.1 (2.5–3.6) L/min per m^2, pulmonary vascular resistance was 1.8 (1.4–2.3) indexed Woods units, transpulmonary gradient was 4 (3.5–5.9) mm Hg, peak ventricular systolic pressure was 102 (88–114) mm Hg, and ventricular end-diastolic pressure was 10 (8–12) mm Hg. Among these variables, the RV group had a lower peak ventricular systolic pressure as compared with LV group (94 [86–109] mm Hg versus 110 [99–122] mm Hg, $P=0.015$). Other variables were not significantly different between the groups. A higher peak ventricular systolic pressure correlated with having a better GCS ($R^2=0.39$, $P=0.014$) and a lower EDV_i ($R^2=0.42$, $P=0.001$). Fontan baffle pressure did not show a significant correlation with ventricular size, EF, strain, or stress. Demographic characteristics and CMR data for this subgroup of patients are summarized in Table I in the Data Supplement.

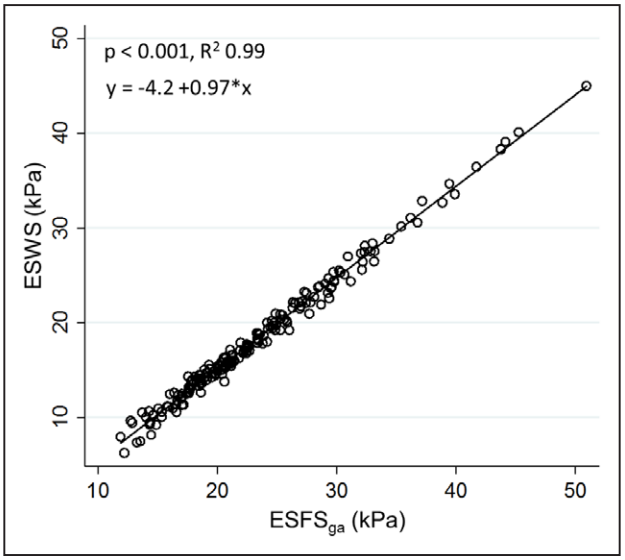

Figure 2. Correlation between end-systolic wall stress (ESWS) and global average midwall end-systolic fiber stress ($ESFS_{ga}$).

Outcomes

Exercise testing data within 2 years of the CMR were available in 81 patients (28 RV, 53 LV). The median gap between the exercise testing and CMR was 61 (0–343) days. There were no significant differences in percent predicted work rate (LV: 68% [54%–76%] versus RV: 72% [59%–93%], *P*=0.125), percent predicted peak Vo_2 (LV: 65% [52%–74%] versus RV: 67% [54%–83%], *P*=0.262), or VE/Vco_2 slope (LV: 32 [29–36] versus RV: 32 [28–35], *P*=0.708) between the groups. There was a linear decline in percent predicted peak Vo_2 with decreasing EF (R^2=0.29, *P*=0.009); however, no significant relationship was observed between percent predicted peak Vo_2 and $ESFS_{ga}$ (*P*=0.145), GLS (*P*=0.726), or GCS (*P*=0.421). Demographic characteristics and CMR data for this subgroup of patients are summarized in Table II in the Data Supplement.

With a median follow-up period of 6.2 (3.6–9.5) years, 24 (12%) of the patients met the composite outcome with 20 deaths, 2 heart transplantations, and 2 heart transplant listings. In the RV group, 15 of 92 (16%) patients had the outcome as compared with 9 of 101 (9%) in the LV group. LV group had higher freedom from the composite outcome as compared with the RV on Kaplan Meier survival analysis with log-rank test (Figure 3). Of the measured variables, a higher EDV_i and a worse GCS were associated with death or needing transplant on univariate analysis (EDV_i: 111 [87–175] mL/$BSA^{1.3}$ versus 91 [76–117] mL/ $BSA^{1.3}$, *P*=0.004; GCS: −17% [−22% to −12%] versus −23% [−26% to −19%], *P*=0.010).

DISCUSSION

This study assessed the relationships between ventricular morphology, wall and fiber stress, and strain in patients after the Fontan operation using CMR. Compared with Fontan patients with LV morphology, those with RV morphology showed a higher rate of death/transplantation, higher ventricular volumes, lower mass-to-volume ratio, and lower circumferential fiber shortening. Interestingly, the longitudinal shortening, as assessed by GLS, was similar between the groups. These data on ventricular mechanics may help explain the suboptimal adaptation of the RV as a systemic ventricle. The association of transplant-free survival with ventricular dilation and decreased circumferential strain in this population was reaffirmed.[25]

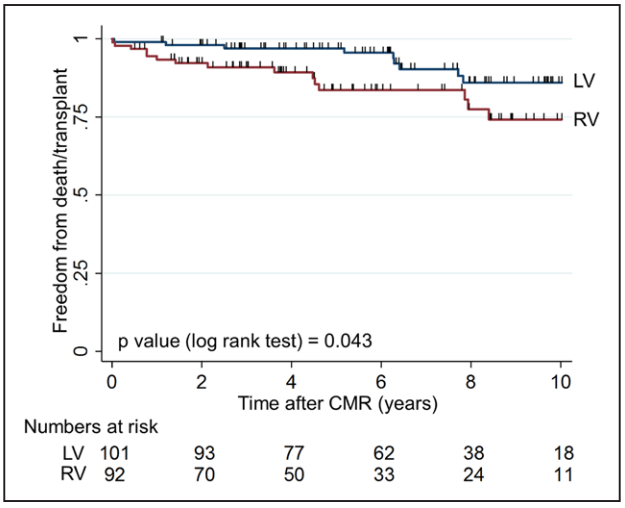

Figure 3. Kaplan Meier curves showing freedom from the composite outcome of death, transplantation, or transplant listing between left ventricular (LV) and right ventricular (RV) groups.
CMR indicates cardiac magnetic resonance.

As a measure of myocardial afterload, wall, and fiber stresses are important determinants of ventricular function, hypertrophy, and oxygen consumption. Many of the mathematical models used for calculation of wall stress are based on the assumption of a spherical or prolate ellipsoid shape to account for LV morphology. These equations do not consider the presence of a second ventricle and have been developed through the assumption that the RV exerts no impact on the LV wall stress. Despite these limitations, increased LV wall stress, measured noninvasively, has been associated with adverse outcomes in adults with ischemic heart disease.[26] In a recent large study of 1768 asymptomatic adults enrolled in the MESA (Multi-Ethnic Study of Atherosclerosis), a higher ESWS (calculated using a similar method as in the present study) was associated with a higher rate of incident heart failure.[27] Its prognostic ability, however, was superseded by GCS in a multivariable analysis. The assumptions in these techniques may be even more important in the Fontan circulation where ventricular shape can be highly variable. Nevertheless, it is important to note that the mean LV ESWS in the MESA cohort was 8.9±2.5 kPa, which is dramatically lower than 16.5±6 kPa for the LV group and 19.2±7 kPa for the RV group in the present study. The purpose in using the Regen model to derive $ESFS_{ga}$ in addition to the ESWS in the current study is that it was specifically formulated to allow calculation of global average wall and fiber stress that is accurate for chambers of any shape and fiber orientation and makes no assumptions about the impact of a second ventricle.[21,28]

The RV group in the current study had higher wall and fiber stresses despite a lower BP. Because stress is a function of pressure×(volume/mass), mathematically the higher volume/mass accounts for the elevated stress. The difference between wall and fiber stress is that wall stress does not take into account the fact that radial stress inhibits fiber shortening, and therefore underestimates the forces opposing fiber shortening. The Regen equations incorporate these forces, as reflected in the fact that fiber stress is invariably higher than wall stress. A worse GCS but a similar GLS in the RV group in comparison to the LV group likely results from differences in

fiber arrangement and preferred direction of shortening. The normal RV myofiber architecture and orientation are characterized by more longitudinal and fewer circumferentially oriented fibers than is observed in the LV, which is mechanically disadvantageous for pressure generation.[29] Dilated RVs also had a lower GCS than nondilated RVs. Taken together, these observations suggest that compared with the LV, the RV adapts less well to the substantial increase in hemodynamic load associated with the Fontan circulation.

Ventricular dilatation was associated with death and heart transplantation in this study, a finding similar to previously published data from an overlapping cohort from our institution.[15] This is not unique to the Fontan circulation as dilation of the systemic ventricle is an established marker of worse prognosis in several conditions, including dilated cardiomyopathy and mitral and aortic regurgitation.[30] In contrast to acquired myocardial disorders, the systemic single ventricle is exposed to abnormal hemodynamic stress beginning from prenatal life, which may predispose it to early failure. Indeed, the RV group had a higher rate of heart transplantation or death compared with the LV group in the current cohort. The RV is particularly at risk of failure as it has evolved to support the low-resistance, high-capacitance pulmonary circulation. Higher rate of AVV regurgitation may contribute to ventricular dilation in the RV group. Dilatation, along with an inadequate increase in ventricular mass predisposes RVs to higher wall stress compared with LVs; however, the exact mechanisms underlying worse adaptation of the RV in the Fontan circulation remain largely unknown.

Study Limitations

This study used mathematical models to estimate average systolic wall stress inside a chamber that is often quite irregularly shaped with nonuniform wall thickness. Although global average wall stress was higher in the RV group, this study does not provide regional information. Higher volume/mass is mathematically responsible for a higher wall and fiber stress in the RV group, but the underlying mechanisms for these abnormalities remain unknown. Mean cuff arm blood pressure was used as a surrogate for end-systolic ventricular pressure. An accurate ventricular pressure can be obtained invasively; however, the retrospective nature of this analysis precluded this type of assessment. It is important to note that there is no available method to directly measure wall stress invasively, including open chest or isolated muscle preparations.[31] Patients with pacemakers and defibrillators were excluded from this study as they remain a relative contraindication to a CMR examination. Referral bias for CMR testing may mean that sicker and more symptomatic patients are overrepresented in this cohort. This was a cross-sectional analysis that precludes evaluation of the temporal relationships between ventricular dilation, hypertrophy, and dysfunction. The time gap between the exercise testing and catheterization and CMR was relatively long (up to 2 years) considering the average age of ≈16 years in this cohort. As a result, bias arising from this time gap cannot be completely excluded. The catheterization and exercise testing subgroups may be also biased subsets of the larger population, and the power to detect difference between LV and RV morphology within these subgroups is more limited.

Conclusions

Compared with Fontan patients with LV morphology, those with RV morphology have higher end-systolic wall and fiber stress, a higher rate of ventricular dilation, lower circumferential fiber shortening, and similar longitudinal shortening. Difference in myofiber architecture may contribute to suboptimal adaptation of the RV as a systemic ventricle. RV morphology, ventricular dilation, and worse circumferential strain are associated with death or transplantation in this population.

ARTICLE INFORMATION

Received May 30, 2017; accepted May 10, 2018.

The Data Supplement is available at http://circimaging.ahajournals.org/lookup/suppl/doi:10.1161/CIRCIMAGING.117.006738/-/DC1.

Correspondence

Sunil J. Ghelani, MD, Department of Cardiology, Boston Children's Hospital, 300 Longwood Ave, Boston, MA 02115. E-mail sunil.ghelani@cardio.chboston.org

Affiliations

Department of Cardiology, Boston Children's Hospital, MA. Department of Pediatrics, Harvard Medical School, Boston, MA.

Sources of Funding

This study was in part supported by the Higgins Family Noninvasive Cardiac Imaging research funds at Boston Children's Hospital.

Disclosures

None.

REFERENCES

1. Waterhouse BR, Bera KD. Why right is never left: the systemic right ventricle in transposition of the great arteries. *J Physiol*. 2015;593:5039–5041. doi: 10.1113/JP271483.
2. Moons P, Gewillig M, Sluysmans T, Verhaaren H, Viart P, Massin M, Suys B, Budts W, Pasquet A, De Wolf D, Vliers A. Long term outcome up to 30 years after the Mustard or Senning operation: a nationwide multicentre study in Belgium. *Heart*. 2004;90:307–313.
3. Gentles TL, Mayer JE Jr, Gauvreau K, Newburger JW, Lock JE, Kupferschmid JP, Burnett J, Jonas RA, Castañeda AR, Wernovsky G. Fontan operation in five hundred consecutive patients: factors influencing early and late outcome. *J Thorac Cardiovasc Surg*. 1997;114:376–391.
4. Deal BJ, Costello JM, Webster G, Tsao S, Backer CL, Mavroudis C. Intermediate-term outcome of 140 consecutive Fontan conversions with

arrhythmia operations. *Ann Thorac Surg*. 2016;101:717–724. doi: 10.1016/j.athoracsur.2015.09.017.
5. Pundi KN, Johnson JN, Dearani JA, Pundi KN, Li Z, Hinck CA, Dahl SH, Cannon BC, O'Leary PW, Driscoll DJ, Cetta F. 40-year follow-up after the Fontan operation: long-term outcomes of 1,052 patients. *J Am Coll Cardiol*. 2015;66:1700–1710. doi: 10.1016/j.jacc.2015.07.065.
6. Khairy P, Fernandes SM, Mayer JE Jr, Triedman JK, Walsh EP, Lock JE, Landzberg MJ. Long-term survival, modes of death, and predictors of mortality in patients with Fontan surgery. *Circulation*. 2008;117:85–92. doi: 10.1161/CIRCULATIONAHA.107.738559.
7. Julsrud PR, Weigel TJ, Van Son JA, Edwards WD, Mair DD, Driscoll DJ, Danielson GK, Puga FJ, Offord KP. Influence of ventricular morphology on outcome after the Fontan procedure. *Am J Cardiol*. 2000;86:319–323.
8. Khairy P, Poirier N, Mercier LA. Univentricular heart. *Circulation*. 2007;115:800–812. doi: 10.1161/CIRCULATIONAHA.105.592378.
9. Anderson PA, Sleeper LA, Mahony L, Colan SD, Atz AM, Breitbart RE, Gersony WM, Gallagher D, Geva T, Margossian R, McCrindle BW, Paridon S, Schwartz M, Stylianou M, Williams RV, Clark BJ III; Pediatric Heart Network Investigators. Contemporary outcomes after the Fontan procedure: a Pediatric Heart Network multicenter study. *J Am Coll Cardiol*. 2008;52:85–98. doi: 10.1016/j.jacc.2008.01.074.
10. McGuirk SP, Winlaw DS, Langley SM, Stumper OF, de Giovanni JV, Wright JG, Brawn WJ, Barron DJ. The impact of ventricular morphology on mid-term outcome following completion total cavopulmonary connection. *Eur J Cardiothorac Surg*. 2003;24:37–46.
11. Ohuchi H, Kagisaki K, Miyazaki A, Kitano M, Yazaki S, Sakaguchi H, Ichikawa H, Yamada O, Yagihara T. Impact of the evolution of the Fontan operation on early and late mortality: a single-center experience of 405 patients over 3 decades. *Ann Thorac Surg*. 2011;92:1457–1466. doi: 10.1016/j.athoracsur.2011.05.055.
12. Tweddell JS, Nersesian M, Mussatto KA, Nugent M, Simpson P, Mitchell ME, Ghanayem NS, Pelech AN, Marla R, Hoffman GM. Fontan palliation in the modern era: factors impacting mortality and morbidity. *Ann Thorac Surg*. 2009;88:1291–1299. doi: 10.1016/j.athoracsur.2009.05.076.
13. Alter P, Rupp H, Stoll F, Adams P, Figiel JH, Klose KJ, Rominger MB, Maisch B. Increased end diastolic wall stress precedes left ventricular hypertrophy in dilative heart failure–use of the volume-based wall stress index. *Int J Cardiol*. 2012;157:233–238. doi: 10.1016/j.ijcard.2011.07.092.
14. Morton G, Schuster A, Jogiya R, Kutty S, Beerbaum P, Nagel E. Inter-study reproducibility of cardiovascular magnetic resonance myocardial feature tracking. *J Cardiovasc Magn Reson*. 2012;14:43. doi: 10.1186/1532-429X-14-43.
15. Rathod RH, Prakash A, Kim YY, Germanakis IE, Powell AJ, Gauvreau K, Geva T. Cardiac magnetic resonance parameters predict transplantation-free survival in patients with Fontan circulation. *Circ Cardiovasc Imaging*. 2014;7:502–509. doi: 10.1161/CIRCIMAGING.113.001473.
16. Rathod RH, Prakash A, Powell AJ, Geva T. Myocardial fibrosis identified by cardiac magnetic resonance late gadolinium enhancement is associated with adverse ventricular mechanics and ventricular tachycardia late after Fontan operation. *J Am Coll Cardiol*. 2010;55:1721–1728. doi: 10.1016/j.jacc.2009.12.036.
17. Sluysmans T, Colan SD. Theoretical and empirical derivation of cardiovascular allometric relationships in children. *J Appl Physiol (1985)*. 2005;99:445–457. doi: 10.1152/japplphysiol.01144.2004.
18. Grosse-Wortmann L, Al-Otay A, Yoo SJ. Aortopulmonary collaterals after bidirectional cavopulmonary connection or Fontan completion: quantification with MRI. *Circ Cardiovasc Imaging*. 2009;2:219–225. doi: 10.1161/CIRCIMAGING.108.834192.
19. Prakash A, Rathod RH, Powell AJ, McElhinney DB, Banka P, Geva T. Relation of systemic-to-pulmonary artery collateral flow in single ventricle physiology to palliative stage and clinical status. *Am J Cardiol*. 2012;109:1038–1045. doi: 10.1016/j.amjcard.2011.11.040.
20. Mirsky I. Left ventricular stresses in the intact human heart. *Biophys J*. 1969;9:189–208. doi: 10.1016/S0006-3495(69)86379-4.
21. Regen DM. Calculation of left ventricular wall stress. *Circ Res*. 1990;67:245–252.
22. Colan SD, Fujii A, Borow KM, MacPherson D, Sanders SP. Noninvasive determination of systolic, diastolic and end-systolic blood pressure in neonates, infants and young children: comparison with central aortic pressure measurements. *Am J Cardiol*. 1983;52:867–870.
23. Ghelani SJ, Harrild DM, Gauvreau K, Geva T, Rathod RH. Echocardiography and magnetic resonance imaging based strain analysis of functional single ventricles: a study of intra- and inter-modality reproducibility. *Int J Cardiovasc Imaging*. 2016;32:1113–1120. doi: 10.1007/s10554-016-0882-4.
24. IBM. Testing the Equality of Regression Slopes Among Groups - United States [Internet]. https://www-304.ibm.com/support/docview.wss?uid=swg21476883. Accessed January 26, 2010.
25. Ghelani SJ, Harrild DM, Gauvreau K, Geva T, Rathod RH. Comparison between echocardiography and cardiac magnetic resonance imaging in predicting transplant-free survival after the Fontan operation. *Am J Cardiol*. 2015;116:1132–1138. doi: 10.1016/j.amjcard.2015.07.011.
26. Clerfond G, Bière L, Mateus V, Grall S, Willoteaux S, Prunier F, Furber A. End-systolic wall stress predicts post-discharge heart failure after acute myocardial infarction. *Arch Cardiovasc Dis*. 2015;108:310–320. doi: 10.1016/j.acvd.2015.01.008.
27. Choi EY, Rosen BD, Fernandes VR, Yan RT, Yoneyama K, Donekal S, Opdahl A, Almeida AL, Wu CO, Gomes AS, Bluemke DA, Lima JA. Prognostic value of myocardial circumferential strain for incident heart failure and cardiovascular events in asymptomatic individuals: the Multi-Ethnic Study of Atherosclerosis. *Eur Heart J*. 2013;34:2354–2361. doi: 10.1093/eurheartj/eht133.
28. Sluysmans T, Sanders SP, van der Velde M, Matitiau A, Parness IA, Spevak PJ, Mayer JE Jr, Colan SD. Natural history and patterns of recovery of contractile function in single left ventricle after Fontan operation. *Circulation*. 1992;86:1753–1761.
29. Colan SD. Ventricular function in volume overload lesions. In: Fogel MA, ed. *Ventricular Function and Blood Flow in Congenital Heart Disease*. Malden, MA: Wiley-Blackwell; 2005:205–222.
30. Nishimura RA, Otto CM, Bonow RO, Carabello BA, Erwin JP III, Guyton RA, O'Gara PT, Ruiz CE, Skubas NJ, Sorajja P, Sundt TM III, Thomas JD; American College of Cardiology/American Heart Association Task Force on Practice Guidelines. 2014 AHA/ACC guideline for the management of patients with valvular heart disease: a report of the American College of Cardiology/American Heart Association Task Force on Practice Guidelines. *J Am Coll Cardiol*. 2014;63:e57–e185. doi: 10.1016/j.jacc.2014.02.536.
31. Colan SD. Assessment of ventricular and myocardial performance. In: Keane JF, et al, eds. *Nadas' Pediatric Cardiology*. Philadelphia, PA: Saunders; 2006:251–273.

Impact of Ventricular Morphology on Fiber Stress and Strain in Fontan Patients

Sunil J. Ghelani, Steven D. Colan, Nina Azcue, Ellen M. Keenan, David M. Harrild, Andrew J. Powell, Tal Geva and Rahul H. Rathod

Circ Cardiovasc Imaging. 2018;11:
doi: 10.1161/CIRCIMAGING.117.006738
Circulation: Cardiovascular Imaging is published by the American Heart Association, 7272 Greenville Avenue, Dallas, TX 75231

Print ISSN: 1941-9651. Online ISSN: 1942-0080

Supplemental material

Table 1. Patient characteristics for subjects with available catheterization data.

	All Patients (n = 70)	**RV group (n = 38)**	**LV group (n = 32)**	**p value**
Age at Fontan (y)	3 [2.3, 5.1]	2.7 [2.3, 4.1]	3.6 [2.3, 7]	0.126
Age at CMR (y)	15 [8, 23]	11 [5, 18]	18 [11, 25]	**0.022**
BSA (m^2)	1.5 [0.8, 1.7]	1.3 [0.7, 1.7]	1.6 [1.3, 1.7]	**0.048**
Heart rate (bpm)	83 [64, 102]	88 [72, 76]	80 [60, 98]	0.083
EDV_i ($ml/BSA^{1.3}$)	108 [80, 139]	114 [88, 163]	89 [74, 118]	**0.007**
ESV_i ($ml/BSA^{1.3}$)	48 [33, 71]	56 [38, 82]	40 [30, 61]	**0.033**
$Mass_i$ ($gram/BSA^{1.3}$)	52 [44, 65]	52 [45, 70]	52 [41, 60]	0.472
Mass-to-volume ratio	0.52 [0.40, 0.61]	0.47 [0.35, 0.56]	0.55 [0.45, 0.72]	**0.011**
EF (%)	52 [47, 59]	51 [47, 59]	52 [46, 59]	0.906
ESWS (kPa)	15 [13, 23]	17 [14, 26]	14 [12, 22]	0.125
$ESFS_{ga}$ (kPa)	20 [17, 28]	22 [18, 30]	19 [17, 27]	0.183
GCS (%)	-23 [-26, -18]	-21 [-24, -18]	-25 [-28, -20]	**0.011**
GLS (%)	-17 [-20, -12]	-18 [-21, -13]	-16 [-18, -12]	0.113

Abbreviations: *LV* left ventricle, *RV* right ventricle, EDV_i indexed ventricular end-diastolic volume, ESV_i indexed ventricular end-systolic volume, $Mass_i$ indexed ventricular mass, *EF* ventricular ejection fraction, *ESWS* end-systolic wall stress, $ESFS_{ga}$ global average mid-wall end-systolic fiber Stress, *GCS* global circumferential strain, *GLS* global longitudinal strain

Table 2. Patient characteristics for subjects with available exercise testing data.

	All Patients (n = 70)	**RV group (n = 38)**	**LV group (n = 32)**	**p value**
Age at Fontan (y)	4 [2, 8]	4 [2, 8]	4 [2, 8]	0.509
Age at CMR (y)	21 [16,28]	18 [15, 23]	23 [16, 29]	0.089
BSA (m^2)	1.6 [1.5, 1.9]	1.6 [1.5, 1.8]	1.7 [1.5, 1.9]	0.456
Heart rate (bpm)	80 [65, 88]	82 [64, 89]	80 [65, 87]	0.643
EDV_i ($ml/BSA^{1.3}$)	83 [65, 112]	101 [80, 119]	81 [71, 94]	**0.003**
ESV_i ($ml/BSA^{1.3}$)	39 [32, 55]	43 [34, 67]	38 [29, 52]	**0.036**
$Mass_i$ ($gram/BSA^{1.3}$)	47 [40, 58]	45 [39, 61]	48 [41, 58]	0.340
Mass-to-volume ratio	0.57 [0.47, 0.67]	0.47 [0.39, 0.54]	0.59 [0.53, 0.70]	**<0.001**
EF (%)	54 [47, 59]	54 [44, 58]	54 [47, 60]	0.620
ESWS (kPa)	17 [13, 20]	19 [14, 22]	14 [13, 17]	**0.011**
$ESFS_{ga}$ (kPa)	21 [17, 26]	24 [19, 27]	20 [17, 23]	**0.015**
GCS (%)	-24 [-28, -19]	-21 [-24, -16]	-25 [-29, -21]	0.080
GLS (%)	-18 [-21, -12]	-21 [-25, -13]	-16 [-19, -12]	**0.019**

Abbreviations: *LV* left ventricle, *RV* right ventricle, EDV_i indexed ventricular end-diastolic volume, ESV_i indexed ventricular end-systolic volume, $Mass_i$ indexed ventricular mass, *EF* ventricular ejection fraction, *ESWS* end-systolic wall stress, $ESFS_{ga}$ global average mid-wall end-systolic fiber Stress, *GCS* global circumferential strain, *GLS* global longitudinal strain